

INTERNATIONAL JOURNAL OF MULTIDISCIPLINARY RESEARCH

IN SCIENCE, ENGINEERING, TECHNOLOGY AND MANAGEMENT

Volume 11, Issue 5, May 2024



INTERNATIONAL
STANDARD
SERIAL
NUMBER
INDIA

Impact Factor: 7.802



+91 99405 72462



+9163819 07438



ijmrsetm@gmail.com



www.ijmrsetm.com

Photo Response of Organic Field Effect Transistor

ANITA RAJ

Department of Physics, Government College, Behror, Rajasthan, India

ABSTRACT: Over the past twenty years, research into the applications of OSCs has intensified rapidly. Their though electron mobility is much lower than that of typical semiconductors, OSCs show promise in low- cost, flexible, lightweight, shock resistance, transparency and environmentally-friendly semiconductors Applications. Device Performance have improved in last decades with evolution of device Structures from Single layer to multilayer ambipolar transistors. There are many Studies on Materials systems in a wide variety of applications such as flexible flat -panel displays, Sensors, Photovoltaics, Photo detectors, OLEDs, OFETs and electronics paper.

KEYWORDS: Organic semiconductors devices, organic field effect transistors, organic light emitting diodes, Photo voltaic cells, Silicon, Metal oxide semiconductor FET, organic photo transistors, Thin - film Transistor, Dinaphtho-thieno -thiophene, Poly Methyl Methacrylate, Organic Photovoltaics.

I. INTRODUCTION

Photo sensitive elements based on OTFTs readily integrated into flexible, large - area organic circuits new scope in light sensing application [1]. Polymer dielectrics in OFETs are essential to provide the devices with overall flexibility. ,stretchability, and printability and simultaneously introduce charge interaction on the interface with OSCs[2]. Field effect transistors using dinaphtho[2,3-b:2',3'-f]thieno[3,2-b] thiophene [DNNT] as an OSCs can be operated below -5V with a high mobility of 0.53 cm²/(V.s). The DNNT transistor showed a good photo response to blue light with a wavelength of 450 nm [3]. The dielectric properties of PMMA gate dielectric & unravel its effect on the OFETs performance environmental *stability*, and photosensitivity [4]. Flexible Organic Photovoltaics (OPVs) are promising power sources for wearable electronics [5]. OFETs have advantages such as low- cost, light- weight, and high flexibility [6]. Photo transistors that can detect optical signals convert optical variation into and electrical signals are one of the major advantages of OFETs. The internal signal amplification function of the transistor device endows photo transistors with high photosensitivity and low noise [7]. Many of these applications requires some sort of sensors capable of extracting data from the environment, such as pressure, temperature, humidity or light, imaging capabilities could potentially have the widest range of applications, they can be used for photography, scanning, object or movement detection. A Flexible Image sensor on substrate using organic photodiode [8].

II. METHODS & MATERIALS

2.1. Fabrication

All transistors and phototransistors were fabricated in the inverted-staggered (bottom-gate, top-contact) configuration on a flexible polyethylene naphthalate (PEN) substrate using a set of 4 high-resolution silicon stencil masks. A thick layer of the high mobility organic semiconductor DNNT was then sublimated through a third stencil mask. Finally, Au source/drain contacts were patterned using a fourth mask. The transistors are illuminated from the top, as the gate metal is opaque. Therefore, light mainly enters the device in the intrinsic transistor area.

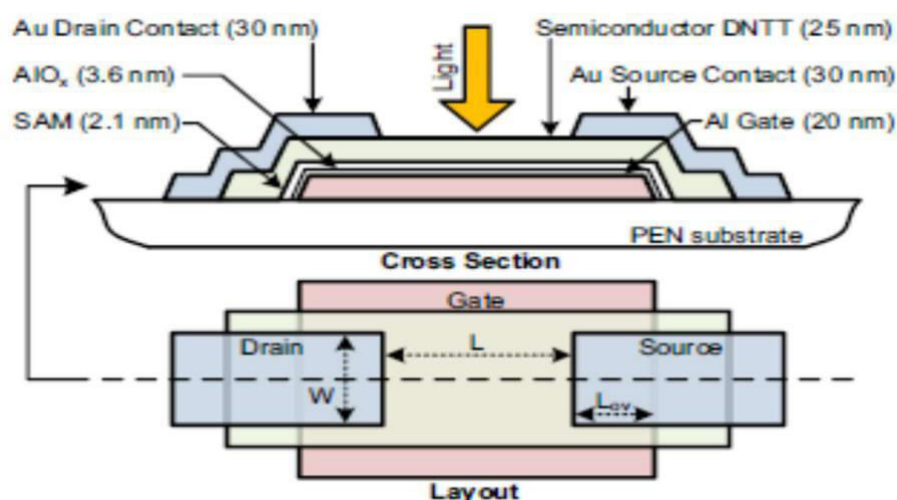


Fig. 1 Cross section and layout of a top-illuminated, inverted-staggered (bottom-gate, top-contact) organic phototransistor

The optical absorption properties of the organic semiconductor DNTT are determined by a transmission measurement. This experiment was performed using a glass substrate with a stack of AlOx (by atomic layer deposition), a SAM and DNTT, and the measured spectrum was referenced against that obtained from a substrate without DNTT. The measured spectrum indicates sensitivity to ultraviolet (UV) and blue illumination.

Under illumination, the p-channel DNTT OPTs show a strong and slow threshold-voltage shift ΔV_{th} towards more positive values, which is attributed to the formation of an additional charge sheet caused by the trapping of photo generated electrons. The trap centres are believed to be Located either in the bulk of the AlOx(which the electrons can reach by tunnelling through thick SAM) or at the interface between the semiconductor and the SAM.

of an additional charge sheet caused by the trapping of photo generated electrons. The trap centres are believed to be Located either in the bulk of the AlOx(which the electrons can reach by tunnelling through thick SAM) or at the interface between the semiconductor and the SAM. Although freshly grown AlOx surfaces have a large density of hydroxyl groups that could potentially act as electron traps, these hydroxyl groups are eliminated during the grafting of the alkylphosphonic acid SAM and are thus unlikely to play a role here, while trapping in the bulk of the semiconductor can be ruled out because it would produce a different response in the channel modulation. In dark conditions, only a negligible ΔV_{th} is observed, the reason being that only few minority charge carriers, i.e., free electrons, are injected into the semiconductor because of the large energy barrier between the Fermi level of the contact metal (Au) and the lowest unoccupied molecular orbital (LUMO) of DNTT, even at a large drain-source voltage V_{ds} . If light with photon energies within the absorption range of the organic semiconductor enters the device, electron hole pairs are created. Dissociation, which can be enhanced with an electrical field, creates additional electrons and holes, possibly increasing the trap rate and thus the shift. In order to achieve reproducible results from subsequent measurements, the devices have to be reset before each measurement. This is done by creating an accumulation channel with a large negative gate-source voltage V_{GS} while applying a small V_{DS} in order to release trapped charges from the dielectric interface. The reset process can take several seconds to minutes, depending on the initial V_{th} displacement caused by illumination or excessive bias stress.

OFET device structures, determined by the position of the contacts (i.e., gate, source, and drain) relative to the organic semiconductor film, are similar to those of inorganic TFTs. The basic structures are either coplanar or staggered. In a coplanar structure, also called bottom-contact structure, the gate, source, and drain contacts are all located on the same side of the organic semiconductor film, as shown in Figure 2.1(a) and (c).

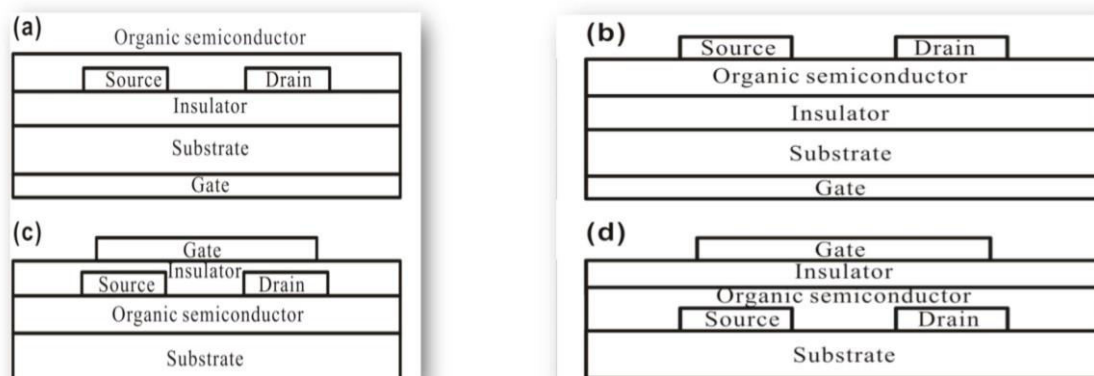


Fig: 2.1 Device structures of OFETs

In a staggered structure, also called top-contact structure, the gate contact is on the opposite side of the organic semiconductor film from the source and drain contacts, as shown in Figure 2.1(b) and (d).

Each structure has two different configurations depending on the position of the gate contact, on the bottom side (bottom-gate or inverted) [Figure 2.1(a) and (b)] or the top side (top-gate) [Figure 2.1(c) and (d)] of the organic semiconductor film, respectively.

Top-gate device structures:

Top-gate device structures as shown in Figure 2.1(c) and (d) have been applied to fabricate polymer TFTs, but have not been widely used in the fabrication of OFETs. The electrical performance of OFET devices with a top-gate structure can be significantly degraded during the deposition process of the top electrodes, and the film growth can be disturbed at the interface of organic semiconductor/metal contacts. Inverted-coplanar device structure (bottom-contact) and inverted-staggered device structure top-contact:

In bottom-contact OFET devices, the organic semiconductor is deposited on to the gate insulator and source/drain contacts.

In top-contact OFET devices, the source/drain contacts are usually deposited on the organic semiconductor through a shadow mask. To facilitate the evaluation of new organic semiconductor materials, heavily n-doped silicon (n^{++} -Si) wafer as the gate contact and thermal Si as gate insulator are used in these two structures. Source/drain contacts are generally arranged in three ways (standard, corbino, and interdigitated) independent of device structure

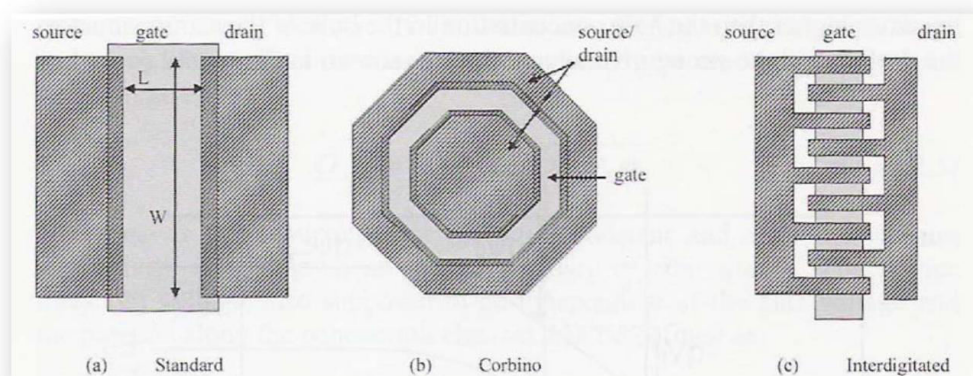


Figure 2.2: Top-views of OFET device structures: (a) Standard OFET; (b) Corbino OFET; (c) Interdigitated OFET

IV. RESULTS & DISCUSSION

3.1. Threshold voltage

The basic operation of the field effect transistor relies on the charge density modulation in the active layer and thus its conductivity can be modulated by a voltage applied to the gate

The charges are injected and collected by the source and drain electrodes, respectively. Observable external electrical quantities are: I_{ds} the drain–source current, V_{ds} the drain–source voltage and V_{gs} the gate–source voltage. The leakage currents, such as drain–gate or gate–source, are considered zero.

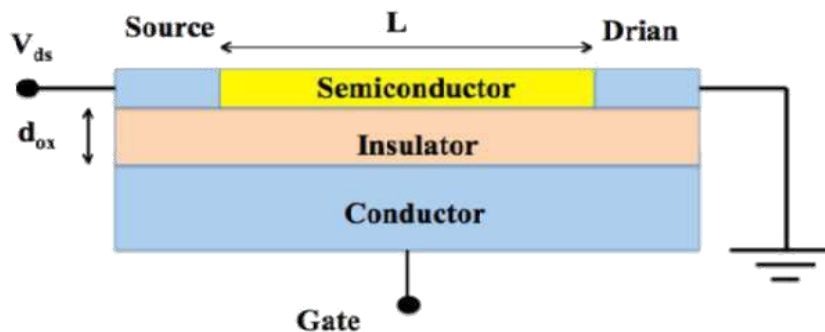


Fig: Schematics of OFET

In a thin-film-transistor, or in general an accumulation-type FET, all induced charge is necessarily close to the insulator and the charge–voltage relation is always simply

$$\rho(x) = V(x) - V_g \cdot C_{ox} \quad ()$$

$$\text{Where } C_{ox} = \epsilon_{ox}/d_{ox}$$

With ρ and V the local charge per area and voltage in the channel, respectively.

This charge in a TFT might still be either mobile or immobile, though It is easy to show that the equation for currents of a MOSFET is also applicable to OFETs. The density of charges p inside the channel varies from one electrode (“source”, $x = 0$) to the other (“drain”, $x = L$). To calculate the currents through the device, we have to understand that, locally, the current $I_x(x)$ at a given point x in the channel is equal to the local induced charge, $C_{ox}[(V_g - V_t) - V(x)]$, multiplied by the carrier mobility μ , the field felt by the charges, $dV(x)/dx$ and the channel width W . In other words, we have the following differential equation

$$I_x(x) = qWp(x)\mu \frac{dV(x)}{dx} \quad ()$$

$$\rho(x) = \frac{C_{ox}[V(x) - (V_g - V_{Th})]}{q} \quad ()$$

V_{Th} is the threshold voltage the threshold voltage can only deviate from zero in the presence of traps. With boundary conditions $V(0)=0$, $V(L)=V_{ds}$, and $I_x(x)=I_{ds}$ for all x , the solution is

$$I_{ds} = (W/L)C_{ox}\mu [(V_g - V_{Th})V_{ds} - 0.5 \cdot (V_{ds})^2] \quad ()$$

V_{ds} and V_g both negative. The equation is valid up to $V_{ds} = V_g - V_{Th}$. After that, saturation starts in a region close to the drain is below threshold voltage and is devoid of charges. When the subthreshold conductivity is (close to) zero this region can be infinitely small and still absorb all of the above-saturation voltage $V_{ds} = (V_g - V_{Th})$. In this way, the charge and voltage distribution across the device (except for an infinitely thin zone) is independent of the drain–source voltage and hence the current is constant at

$$I_{ds} = 0.5(W/L)\mu C_{ox} (V_{Th} - V_g)^2 \quad ()$$

When the sub-threshold conductivity is not zero, the above saturation voltage can only be supported over a finitely thick zone, which depends on the voltage. The remaining voltage drop ($V_{Th} - V_g$) then occurs in a region that is not of constant width but shrinks to $L - 1$ for increased V_{ds} the result is that the saturation current is not constant but continues to increase for higher drain voltages.

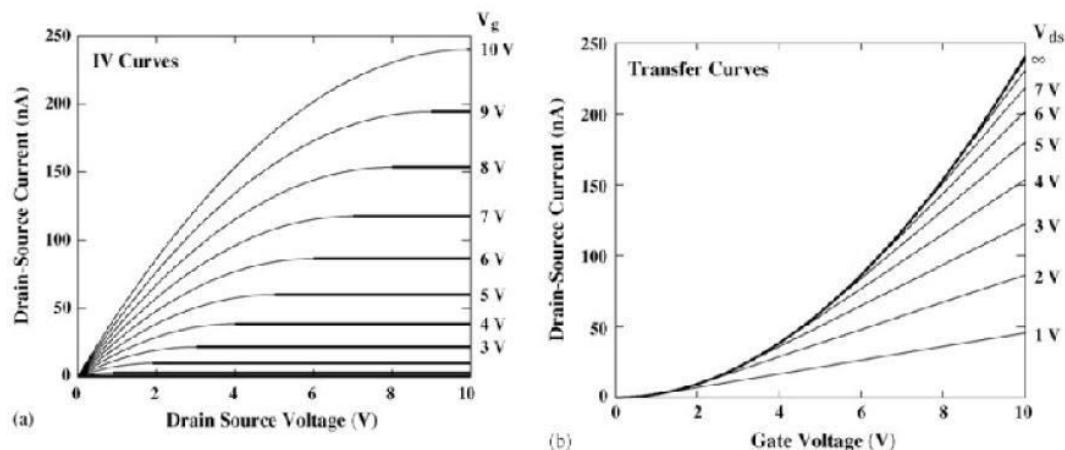


Figure (a) I–V curves (I_{ds} vs V_{ds}) of an ideal thin-film FET resulting from Eq.1.5 (thin lines). (b) Transfer curves for same device. Thick lines indicate the saturation regime.

For low voltages, the quadratic term in V_{ds} disappears from Eq. (1.5) and this is called the linear region. Conventionally, the mobility of an FET is defined via the derivative of a transfer curve (I_{ds} – V_g). Using Eq. (1.5) for small V_{ds}

$$\mu_{FET} = - \frac{L}{WC_{ox}V_{ds}} \frac{\partial I_{ds}}{\partial V_g}$$

3.2. Parameter dependencies:

This section discusses how the light-induced ΔV_{th} is affected by various parameters, such as biasing conditions, integration time, wavelength and power of the incoming light, and the channel length of the transistor. During illumination, V_{GS} has a large impact on ΔV_{th} as it can attract electrons to or repel them from the dielectric interface. A large positive V_{GS} during illumination (for a certain integration time t_{int}) produces the fastest positive ΔV_{th} , whereas a large negative V_{GS} helps with returning the device to the initial state. It has to be noted that during illumination with a large positive V_{GS} , no V_{DS} should be applied to achieve a homogeneous field distribution and trapping throughout the channel, whereas during reset, a small V_{DS} helps with supplying holes for recombination with the released electrons. Fig.3 shows how the transfer characteristics of a DNTT OPT (channel length $L=10$ μm , width $W=1000$ μm) shift as a result of illumination for various integration times from 0 to 360 s. During integration, V_{GS} and V_{DS} are held constant, and the transistor is illuminated with light having a wavelength of $\lambda = 461$ nm and an optical power of $P_{opt} = 66$ nW. During read-out, V_{DS} is set to -1.5 V. The threshold voltage shifts by approximately 2 V from the initial state in the dark at to before saturating after a time t_{sat} . The V_{th} extracted after various integration times is shown in the inset in Fig.3. An exponential fit can be applied according to the following equation:

$$V_{th}(t_{in}) = \Delta V_{th, sat} \exp(-t_{int}/\tau) + V_{th, sat} \quad ()$$

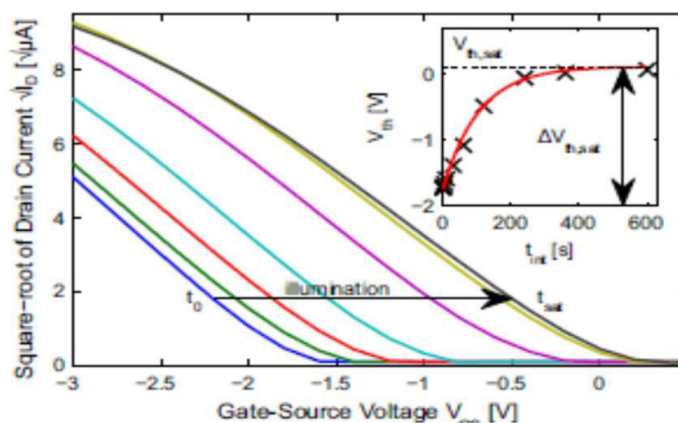


Fig. 3. Light-induced threshold-voltage shift in an organic phototransistor. Each of the transfer curves was measured after a certain integration time t_{int} under illumination. After each measurement, a reset phase was applied, that recovers the original V_{th} . Inset: The exponential dependence of V_{th} on t_{int} indicates that the process is trap-related. The threshold-voltage shift eventually saturates.

Here, V_{th} is expressed by means of $\Delta V_{th,sat}$ which is the total ΔV_{th} from device reset to an equilibrium state under illumination $\Delta V_{th,sat}$. Eq.1 is often used to describe trap related processes and shows that for large integration times and a strong illumination, i.e., when many trappable electrons are present, the process is truly trapping limited. From the exponential fit, a time constant of $\tau = 115$ s is extracted. The characteristically long response time of this trap-related process is partly responsible for the fact that phototransistors are inferior to photodiodes as fast response optical sensors. However, unlike photodiodes, which often require external amplification, phototransistors have a built-in amplification given by their trans conductance g_m . Thus, a useful signal shift is already achieved after integration times much shorter than t_{sat} , as there is no need to wait for complete saturation of V_{th} . The light-induced threshold voltage shift is not always trapping limited, however. For smaller P_{opt} and for shorter t_{int} , ΔV_{th} is in fact limited by optical absorption. Fig 4. Plots the drain current I_D versus P_{opt} in the transistor's saturation regime. When the product of P_{opt} and t_{int} is sufficiently small, the relationship is well-described by a quadratic fit. Within this region, ΔV_{th} increases linearly with P_{opt} due to the additional amount of photo-generated charges per unit area trapped in the AlOx or at the semiconductor-dielectric interface, Q_f

$$\Delta V_{th} = \frac{Q_f}{C_i} + V_{inj} \propto P_{opt}$$

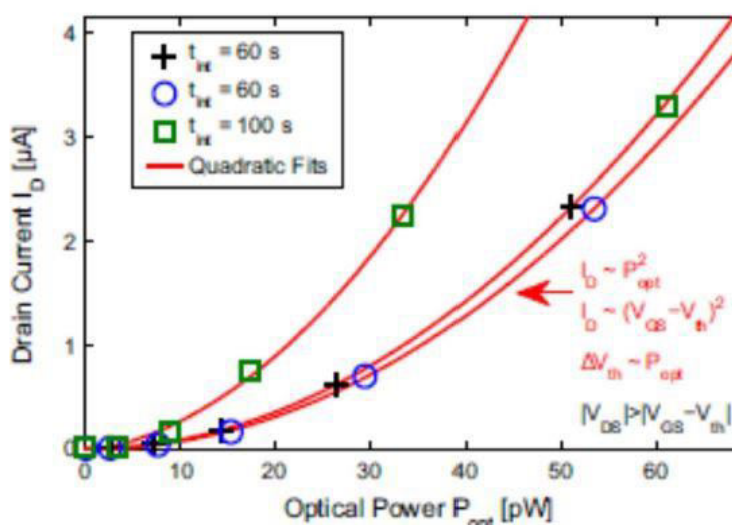


Fig. 4. The drain current measured in the transistor's saturation regime, after various integration times t_{int} under illumination scales quadratically with the optical power P_{opt} when P_{opt} is small and t_{int} is short compared with t_{sat} . The resulting linear relationship between V_{th} and P_{opt} indicates that the process is absorption-limited. In contrast, the process is trapping-limited when P_{opt} is large and t_{int} is long (e.g., 100 s).



Here, C_i is the gate-dielectric capacitance per unit area and V_{inj} is a contribution from the contact resistance. The influence of V_{inj} on ΔV_{th} is neglected here, as ΔV_{th} shows no dependency on V_{DS} . When P_{opt} and t_{int} are large, the relationship between ΔV_{th} and P_{opt} is no longer linear, indicating a transition from the absorption-limited process to the previously mentioned trapping-limited process.

IV. CONCLUSION

The effect of illumination on high-performance, low voltage, DNTT-based OFETs was thoroughly investigated. With proper biasing, the absorption of UV/blue light in the p-channel organic semiconductor DNTT leads to a significant increase in the density of free electrons, which can be trapped in the AlO_x of the gate dielectric or in the semiconductor, at grain boundaries or structural defects reaching the interface of the SAM. This produces a strong but slow threshold voltage shift that translates into a large current modulation through the internal amplification of the OFET. Depending on the channel length of the transistors, the light-induced threshold-voltage shift saturates more or less rapidly, and its final value depends only on the density of trapped electrons. This means that phototransistors can be aggressively scaled down without losing sensitivity, which is an important advantage compared with photodiodes. In principle, it is found that the process is absorption limited for small optical powers and short integration times, while the process becomes trapping limited when the density of light-induced electrons exceeds a certain value. The measured parameter dependencies were used to implement an array of organic phototransistors on a flexible substrate. The electrical performance of OPTs is largely limited by OSCs themselves, posing a challenge to further improve the performance of the devices.

REFERENCES

1. Flexible low-voltage organic phototransistors based on air-stable dinaphtho[2,3-b:20,30-f]thieno[3,2-b]thiophene (DNTT) Johannes Milvich, Tarek Zaki, Mahdieh Aghamohammadi, Reinhold Rödel, Ulrike Kraft, Hagen Klauk, Joachim N. Burghartz.
2. Pursuing Polymer Dielectric Interfacial Effect in Organic Transistors for Photosensing Performance Optimization Xiaohan Wu, Yingli Chu, Rui Liu, Howard E. Katz, and Jia Huang.
3. Flexible and low-voltage organic phototransistors Fanfan Yu, Shaohua Wu, Xiaohong Wang, Guobing Zhang, Hongbo Lu and Longzhen Qiu.
4. Effect of solvent induced dielectric property modulation of poly(methyl methacrylate) insulator on the electrical and photosensing behaviour of p-channel organic transistors D. Panigrahi, S. Kumar, A. Dhar.
5. Alan J. Heeger Department of Physics, Materials Department, Institute for Polymers and Organic Solids, University of California, Santa Barbara, Santa Barbara, California 93106 (Published 20 September 2001)
6. O. Acton, G. G. Ting, P. J. Shamberger, F. S. Ohuchi, H. Ma and A. K. Y. Jen, ACS Appl. Mater. Interfaces, 2010, 2, 511.
7. L. A. Majewski, R. Schroeder, M. Grell, P. A. Glarvey and M. L. Turner, J. Appl. Phys., 2004, 96, 5781.
8. Integration of organic FETs with organic photodiodes for a large area, flexible, and lightweight sheet image scanners, IEEE T. Someya, Y. Kato, S. Iba, Y. Noguchi, T. Sekitani, H. Kawaguchi, T. Sakurai.
9. Other internet source



INTERNATIONAL JOURNAL OF MULTIDISCIPLINARY RESEARCH

IN SCIENCE, ENGINEERING, TECHNOLOGY AND MANAGEMENT



+91 99405 72462



+91 63819 07438



ijmrsetm@gmail.com

www.ijmrsetm.com